Crystallite size dependence of volatilization in matrix-assisted laser desorption ionization

Mehrnoosh Sadeghi, Akos Vertes [*]

Department of Chemistry, George Washington University, Washington, DC 20052, USA

Abstract

During the desorption and ionization processes in matrix-assisted laser desorption ionization (MALDI), the laser beam interacts with different areas of the polycrystalline sample surface varying in crystal size and structure. CCD imaging of dried-droplet and electrospray deposited MALDI samples was used to explore the effect of laser exposure on surface morphology at atmospheric pressure. Crystal size distributions of the sinapinic acid target were examined prior to and after laser irradiation. Image processing and analysis of the difference images revealed the morphological changes in the sample. The results indicate that near-threshold irradiance smaller crystals (~ 2 μm) are completely volatilized by the laser shot, whereas larger crystals undergo layer-by-layer evaporation (peeling). Heat conduction simulations in a finite slab have demonstrated that under similar conditions, the surface temperature of small crystallites increases markedly compared to their larger counterparts. These higher surface temperatures can lead to the selective volatilization of smaller crystallites. This study points to the influence of sample preparation on the crystal size distribution and its consequence on volatilization in MALDI-mass spectrometry (MS). © 1998 Elsevier Science B.V.

Keywords: Matrix-assisted laser desorption ionization (MALDI); Crystal size; Volatilization

1. Introduction

Matrix-assisted laser desorption ionization (MALDI)-mass spectrometry (MS) has become a well-established method for the mass analysis of large molecules. The technique of sample preparation is known to be one of the most significant parameters influencing spectrum quality in this ionization method. Sample preparation in MALDI involves cocrystallization of the guest and matrix molecules from a common solvent at a matrix/guest molar ratio of 1,000–10,000. The first demonstration of protein incorporation into the matrix crystal structure was based on optical microscopy of MALDI samples using dye-stained myoglobin molecules [1,2]. If the concentration of the guest compared to the matrix is too high, the cocrystallization process is disrupted and the spectrum quality deteriorates [3]. Therefore, methods of sample preparation that effectively cocrystallize these molecules are of great importance. The role of sample preparation in MALDI is illustrated by the discrimination of a matrix against some guest molecules due to the lack of efficient incorporation of these molecules into the matrix structure. In addition to the appropriate matrix to guest ratio, the efficient embedding of guest particles during the cocrystallization processes becomes a key

_____
[*] Corresponding author. Tel.: +1-202-994-2717; fax: +1-202-994-5873; e-mail: vertes@gwis2.circ.gwu.edu.

to the success of MALDI. Sample morphology [4] and changes in morphology due to laser exposure [5] are considered critical in determining the ion yield in MALDI-MS of proteins.

Sample morphology is primarily controlled by the method and the conditions of sample preparation. The earliest and most commonly used sample preparation method is the dried-droplet method [6]. This technique forms highly heterogeneous sample surfaces showing large variations in both crystal size and structure. Therefore, during the desorption and ionization process, the laser beam interacts with a large variety of crystallites in this polycrystalline sample [7,8].

The efforts devoted to overcome this problem are mostly directed toward the preparation of more homogeneous samples via the formation of microcrystals [8–15]. The suggested methods include vacuum drying of the samples [12], use of highly volatile solvent for fast evaporation [9], growth and crushing of polycrystalline films on the substrate [10], the formation of highly uniform sample films [11], and spin-coating by the matrix/guest solution [13]. Although electrospray deposited samples have previously been used for desorption studies in laser desorption mass spectrometry (LDMS) [16], only recently has this sample preparation method been applied to MALDI analysis [17]. In the majority of the sample preparation studies, a correlation was found between MALDI signal reproducibility and the homogeneity of the guest distribution in the sample. It has also become apparent that sample morphology is an important factor in the effective desorption and ionization of large molecules.

In an attempt to make these observations quantitative, we studied the crystallite size dependence of volatilization in samples that were prepared by methods used in MALDI (i.e., dried-droplet and electrospray). Earlier calculations of laser heating of finite slabs had indicated the influence of the slab thickness on the surface temperature changes due to laser irradiation [18]. In order to explore the effect of morphology, samples with different crystal size distributions were exposed to single and multiple laser pulses. The effect of the laser–target interaction on the crystal size distributions was examined using CCD imaging. Since the experiments were carried out at atmospheric pressure, some characteristics of

the generated plume (e.g., expansion velocity, plume density, and temperature) can be expected to differ from those in vacuum. However, the present study focuses on the morphological changes of crystallites due to the laser pulses. We believe that the presented results can be correlated with laser volatilization processes observed in vacuum.

2. Experimental

2.1. CCD imaging system

The experimental setup is shown in Fig. 1. A microscope-mounted CCD detector (1530-PUV-1024I, EG&G Princeton Applied Research, Princeton, NJ) was used for the accurate imaging of the crystals. The CCD chip was a Thomson 7896 front-illuminated multiphase pinned (MPP) CCD, with a full image size of 19.4 mm $\times$ 19.4 mm at 1024 $\times$ 1024 pixel resolution. The detector was mounted on a microscope (Olympus CH30, OPELCO, Sterling, VA) by a Nikon 'F' bayonet mount camera coupler (HRX400-NIK, Diagnostic Instruments, Sterling Heights, MI). Using a stage micrometer the field of view under the microscope was measured to be approximately 120 μm $\times$ 120 μm, providing a total magnification (optical and electronic) of $\sim$ 1125.
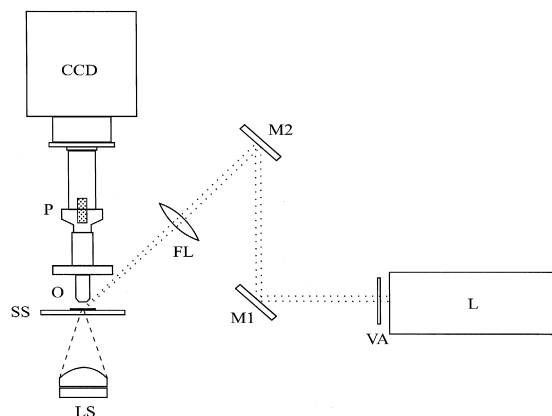

Fig. 1. CCD imaging of laser-irradiated surfaces in reflection geometry. P: 4$\times$ photo eye-piece; O: 40$\times$ objective lens; SS: sample stage; M1 and M2: mirrors; FL: focusing lens; LS: light source; L: laser; VA: variable attenuator.

The sample was illuminated by a nitrogen laser beam (LaserScience, Newton, MA) at 337 nm wavelength under 45° using a focusing lens ($f = 25.4$ mm) (see Fig. 1). The microscope light path and the nitrogen laser beam were aligned in a way that the field of view of the microscope was inside the focal spot of the laser beam, enabling us to monitor the sample before and after interaction with the laser beam. A variable attenuator was used to achieve the appropriate laser irradiance on the sample surface. The energy of the laser pulse was measured with a pyroelectric joule meter (J4-05, Molectron Detector, Portland, OR). Using burn marks on photographic paper, the lower limit of the focal spot diameter on the sample was measured to be ~ 200 μm. The calculated laser irradiance values were treated as higher limits. The calculated laser irradiance in this study varied between 10^6 W/cm^2 and 10^7 W/cm^2, close to the threshold irradiance values for ion generation in MALDI-MS (e.g., $\sim 2 \times 10^6$ W/cm^2 in Ref. [19]). CCD images of the samples were taken alternating between laser shots and imaging steps. A high dynamic range image acquisition software (Version HiDRIS1K, EG&G Instruments Princeton, NJ) was used for data acquisition, display of the images, and data conversion to the appropriate format for later image analysis.

2.2. Sample preparation

The matrices 6-aza-2-thiothymine (ATT) and 3,5-dimethoxy-4-hydroxycinnamic acid (SA) were purchased from Aldrich Chemical (Milwaukee, WI) whereas (α-cyano-4-hydroxycinnamic acid (CHCA) and 2,5-dihydroxybenzoic acid (DHB) were obtained from Sigma Chemical (St. Louis, MO). To vary the surface morphology, the dried-droplet method was applied to both saturated (typically used in MALDI) and more dilute (0.07 M) solutions of SA in a 3:7 (v/v) water and acetonitrile solvent mixture. The samples were prepared by air-drying 2–4 μl of the different solutions on microscope slides (Corning Glass Works, Corning, NY). For the preparation of electrosprayed samples, a 250 μl portion of a solution containing 6.0×10^{-3} M SA in 3:7 (v/v) water/acetonitrile mixture was sprayed on a microscope slide, mounted in front of the ground electrode of the electrospray setup. The microscope slide was

located 2.5–3.5 cm away from the tip of the electrospray capillary of 110–150 μm internal diameter. At 4 kV spray voltage, flow rates of the electrospray varied between 13 μl/min and 27 μl/min. High purity dry nitrogen gas was used as sheet gas

2.3. Image processing and data analysis

Image analysis was performed using the Image-Tool package (Version 1.27) developed by UTH-SCSA. We ensured that spurious objects resulting from noise and optical imperfections in the images were not analyzed in the data. The object analysis results, i.e., the total number, the area, the diameter, and the perimeter of the crystals were exported to a scientific software package (Origin, MicroCal Software, Northampton, MA) and further analyzed there. The analysis of the data showed that the Feret diameter of the crystals was best suited to describe the changes observed as the result of laser–sample interactions. The Feret diameter, d, is defined as the diameter of a circle having the same area, A, as the object: $d = \sqrt{4A/\pi}$. Two parameter lognormal distributions were fitted to the particle diameter, perimeter, and area distributions [20].

3. Theoretical calculations

In order to explore the qualitative consequences of restricted heat conduction in finite crystallites a simple model is created. Individual crystallites of the polycrystalline sample are considered as homogenous infinite slabs of finite thickness. No material transport (i.e., evaporation) or melting are incorporated (most matrix materials sublimate). All material parameters of the slab are considered to be the same throughout. The slab is considered thermally insulated, no heat flow is permitted at the boundaries, therefore $\partial T/\partial z = 0$ at $z = 0$ and $z = L$ (where $\partial T/\partial z$ is the temperature gradient in the z coordinate direction and L is the thickness of the slab). The initial temperature distribution in the slab is considered uniform.

The laser beam is assumed to have cylindrical symmetry and perpendicular incidence on the plane $z = 0$. For a focused beam of fundamental-mode

radiation (TEM_{00}), a Gaussian lateral intensity distribution, $I_a(x, y, t)$, can be applied. With the above simplifications the heat flow equation can be written as:

$$\left(\frac{\partial T}{\partial t} \right) = \kappa \nabla^2 T + \frac{\alpha V_M I_a(x, y, t)}{C_p} e^{-\alpha z} \tag{1}$$

where $\kappa = K V_M / C_p$ is the heat diffusivity, V_M, K, C_p, and α are the molar volume, the thermal conductivity, the specific heat, and the absorption coefficient, respectively. The Green function for this problem is the temperature distribution generated by an instantaneous heat source (e.g., laser) [21]. Based on the Green function solution, the temperature profile for a Gaussian surface source (negligible penetration) can be expressed in cylindrical coordinates:

$$T(r, z, t) = \frac{P_a}{2 K \pi^{3/2}}$$
$$\times \int_0^\delta \exp - \left(\frac{r^2}{\beta^2 + w^2} \right) \gamma_1 \frac{d\beta}{\beta^2 + w^2} \tag{2}$$

where

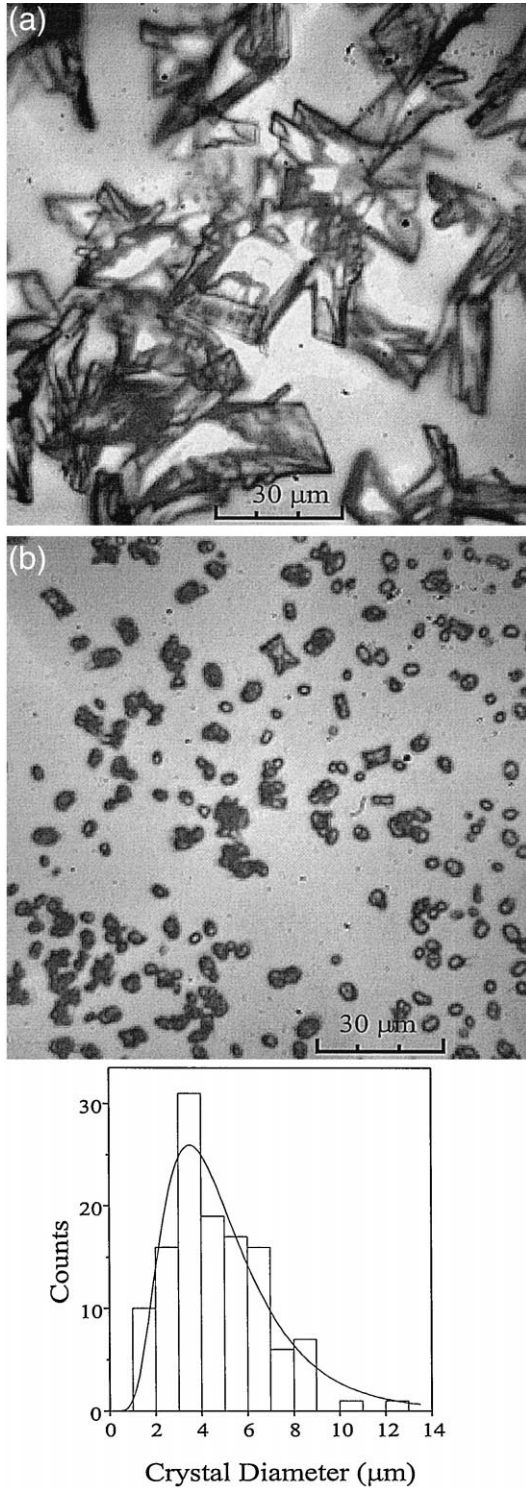$$\gamma_1 = 2 \sum_{n=-\infty}^{\infty} \exp\left(-\frac{(2nL - z)^2}{\beta^2} \right) \tag{3}$$

P_a, w, t_p, and δ are the power for a continuous heat source, laser beam waist, laser pulse duration, and diffusion length, respectively, and $\beta = 2(\kappa|t - t'|)^{1/2}$ [20]. For typical polycrystalline MALDI samples L varies between 10^{-5} cm to 10^{-3} cm. The following laser and material parameter values were used in the calculations: $t_p = 10 \times 10^{-9}$ s, $\delta = 2 \times 10^{-4}$ cm, $w = 0.1$ cm, $K = 10$ (g cm)/(s³ K), $C_p = 1000$ erg/(mole K), $V_M = 100$ cm³/mole [22]. Laser parameters corresponded to typical values for the nitrogen laser, whereas the material parameters were selected to describe an insulator with good absorption characteristics (i.e., matrices). This model was evaluated for maximum surface temperatures of the infinite slabs as a function of their thickness.

4. Results and discussion

In order to investigate the laser volatilization of polycrystalline films and its dependence on crystal-

lite size, we applied reflection geometry irradiation of the samples. Among the matrices studied (SA, DHB, ATT, and CHCA), we found SA to be the most appropriate for this study in terms of the size, shape, and abundance of its crystallites. The preparation of samples using a saturated solution of SA by the dried-droplet method led to crystals of ~ 30 μm in diameter (Fig. 2a). The relatively large size, partial overlap, and small number of crystals in the field of view (120 μm $\times$ 120 μm) did not allow us to efficiently perform image analysis and to use statistical analysis. In order to overcome this problem more dilute solutions were used in the sample preparation, e.g., 0.07 M for SA (see Fig. 2b). It is clearly seen that in the case of the more dilute solution, the average crystal size is smaller. In addition, the crystals are well separated enabling accurate image analysis. The diameter distribution histogram is shown in Fig. 2b. Satisfactory description is obtained by fitting of a lognormal distribution to the histogram with fitting parameters $x_c = 3.49$, $w = 0.496$, and $A = 25.9$.

We also investigated the morphology and its laser induced changes of electrospray deposited samples (Fig. 3a). Compared to the dried-droplet method, in these images the crystallites appear to be more transparent, indicating the formation of thinner plate-like particles. Using these electrosprayed samples the effect of single and multiple laser exposures on sample morphology was investigated. Fig. 3b shows the effect of a single laser shot on the image. The laser beam was aligned on the sample surface at a higher irradiance until the focal area of the beam showed apparent effect on the crystallites in the entire field of view. Then the laser irradiance was decreased to near the MALDI threshold. Since the field of view of the microscope was 120 μm $\times$ 120 μm, and the magnitude of the effect of the laser beam was similar across the field of view, we believe that the laser focal diameter was at least 200 μm, a value similar to the diameter obtained from the burn marks on photographic paper. It is clear that mere visual observation and comparison of Fig. 3a and b do not completely reveal the morphological changes. Since the laser irradiance was kept at a level that only a slight change in morphology was observed after one laser shot ($\sim 10^6$ W/cm²) we applied two complementary methods of images anal-

ysis. Difference images were formed to accentuate the morphological changes as a result of irradiation. In addition, to obtain a quantitative measure of the changes, crystal size (Feret diameter) distributions were calculated before and after laser exposure.

Fig. 4 shows difference images of electrospray deposited and dried-droplet samples. Unthresholded images are the direct result of subtracting images before and after laser exposure. In thresholded images (Fig. 4a), an object threshold was selected and the dynamic range of the image was compressed. Thus, we were able to distinguish the desorbed parts of the crystals from the rest of the image. Black areas indicate the parts eroded by the laser shot. In Fig. 4a for an electrospray deposited sample arrow A shows a difference pattern where due to the interaction with the laser beam a smaller crystallite has completely disappeared. Arrow B shows a location where a crystallite has been reduced in size. It seems that depending on the crystallite size, two different effects are seen: peeling effect for larger crystals and explosion effect on smaller ones. The observed effects also seem to depend on the shape of the crystallites. Some difference patterns appear as complete rings (B). We believe these patterns belonged to crystallites that had a more even thickness and peeled on all surfaces to similar extent. However, other patterns were indicative of uneven material removal probably due to uneven thickness (arrow C). As a consequence of the different thicknesses within crystals certain parts were removed, whereas other parts have remained intact or less eroded.

Studying the unthresholded difference images (Fig. 4b), we noticed some particles with features that set them apart from the difference patterns observed for crystallites that were either completely ablated or peeled by the laser. Fig. 4b shows a difference image of a dried-droplet sample after one laser shot. It seems that in this difference image, the middle part of the crystals has been eroded. We believe that these doughnut-shaped difference patterns belong to crystals that protrude from the surface. The portion of the crystal that is at a higher

Fig. 2. Crystallites in SA sample grown by dried-droplet method (a) from saturated solution; (b) from dilute solution (0.07 M). Feret diameter distribution is provided for crystallites in the (b) image.
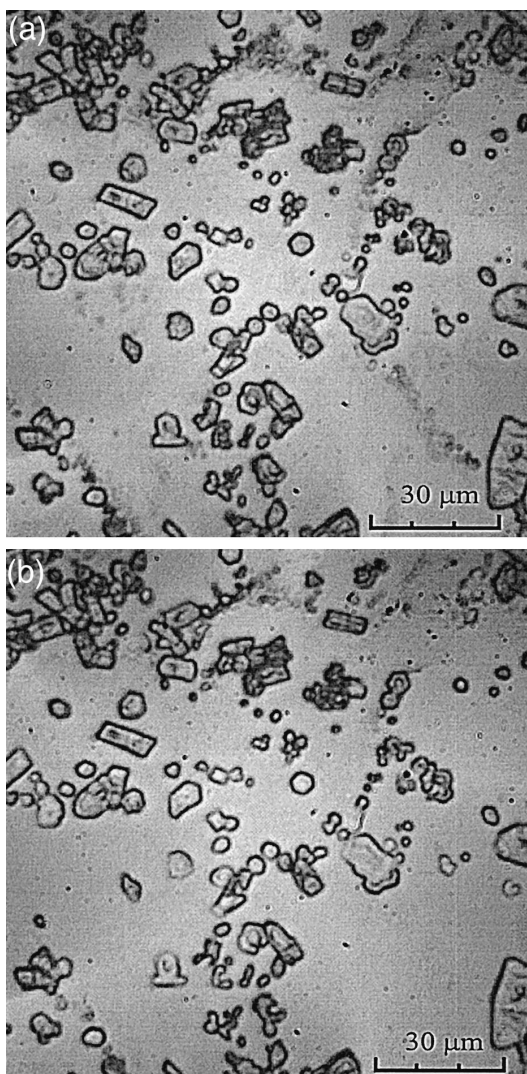
Fig. 3. Laser-induced changes in electrospray deposited sample. The differences between images (a) prior to laser illumination, and (b) after one laser shot are hard to notice.

level than other parts can be ablated by the laser beam and appears in a darker gray color on the difference image (A arrows). In these images, there seems to be no change in the size of the crystal, however, absorbance and thickness changes can be observed. This was more apparent for dried-droplet samples than for the thinner and flat electrospray deposited samples. Unevenly eroded crystals not only appear in the difference images but can also be differentiated from crystals exhibiting the peeling

effect. Thus, to the extent of the dynamic range of the CCD the observation of gray levels in unthresholded images provides information about thickness changes in the sample.

It is known that due to mechanical stress and/or substrate heating in MALDI, crystallites are occa-
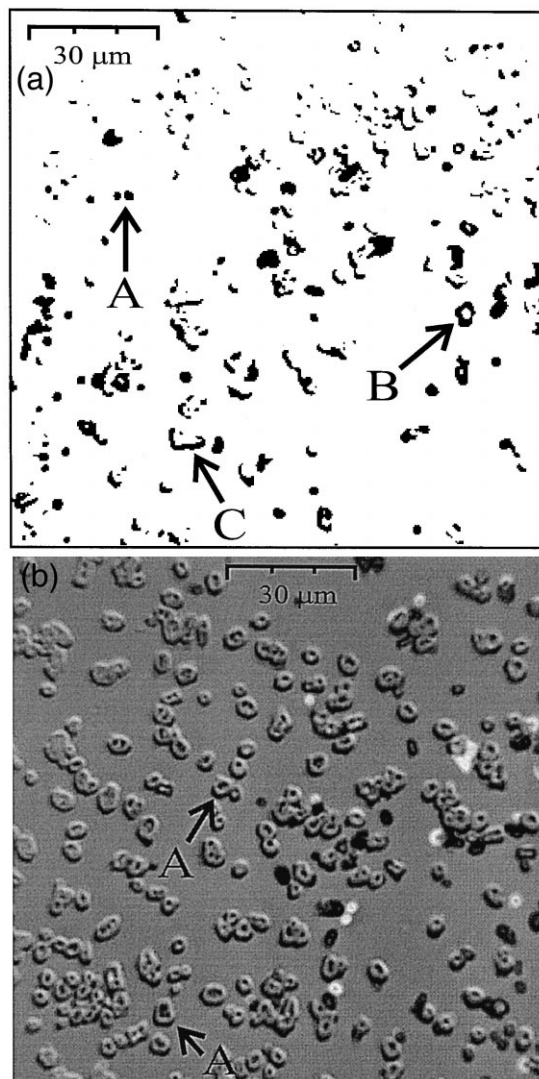

Fig. 4. (a) Thresholded difference image for an electrospray deposited sample. The complete disappearance (e.g., A) and the peeling effect (B, C) are apparent in the image. Ablated particles are shown in solid black, whereas the peeled crystallites are shown as black contours. (b) Unthresholded difference image for a dried-droplet sample. Note the darker areas inside the crystallites that correspond to a thickness change in the z dimension (A).

sionally ejected when the laser beam irradiates the sample. This mechanical ejection of crystallites, however, is not related to the MALDI process. We also observed some cases where crystals that were not present in the field of view prior to laser irradiation appeared in images after laser irradiation (see white spots in Fig. 4b). However, the number of these incidents is very low compared to those that are of our interest. In addition, the peeling effect observed in larger crystals ensures us that the observed phenomenon is indeed related to ablation.

In order to obtain a quantitative measure of erosion, crystal size distribution changes were studied for all amenable images. In addition to the complete volatilization of smaller crystals, in some cases, the crystal size decreases. Size distribution results indicate that the decrease in the population of smaller crystals is greater compared to larger crystals (Fig. 5). Fig. 5a shows the diameter distribution observed for a dried-droplet sample, prior to and after laser irradiation. In both cases lognormal distributions described the data well. The maximum for both distributions appears to be at 7.7 pixels. However, it is apparent that this maximum shows a greater decrease than other parts of the lognormal distribution fitted to the data. This indicates that, despite the full or partial volatilization of almost all sizes of the crystallites, those that are smaller than a critical size show a greater decrease in population due to the laser–sample interaction process.

In the electrospray deposited samples, Fig. 5b, the crystallite sizes seem to spread over a smaller range than in the dried-droplet case, indicating less polydispersity. A shift in the maximum is seen from 4.2 to 6.3 which can be related to the higher incidence of crystallites that were completely removed at around 4.2 pixels. This phenomenon was observed in other data sets as well. Larger crystallites show a peeling effect and become smaller. This results in an increase in the population of medium size crystals after the laser irradiance as seen in Fig. 5b.

It seems that in both cases smaller crystals are predominantly volatilized by the laser beam. By the same token, one can argue that these crystals are probably more involved in the MALDI process. As a result of the laser–sample interaction larger size crystals become smaller. This phenomenon can explain the increase in the abundance of the middle
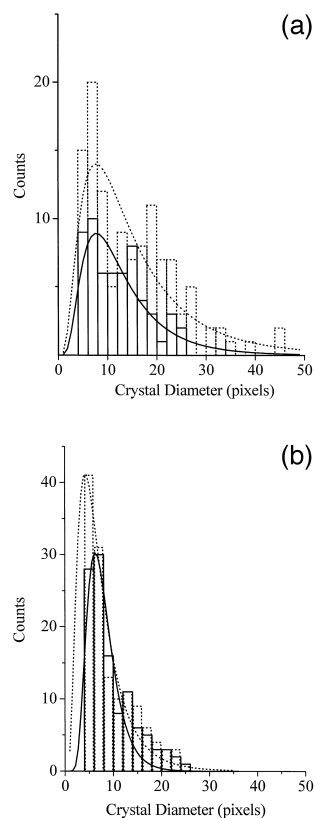

Fig. 5. Comparison of crystal diameter distributions in a MALDI sample before and after laser irradiation for (a) dried-droplet and (b) electrospray deposited samples (- - - before laser exposure; — after laser exposure). All four distributions can be described by lognormal fits. The values for the fitting parameters (x_c, w, and A) for plot (a) are: 7.68, 0.702, and 14.0 prior to laser irradiance and 7.73, 0.594, and 8.91 after laser irradiance, respectively. These values for plot (b) before laser irradiance are: 4.21, 0.619, and 41.2 and after laser irradiance: 6.28, 0.392, and 30.3.

sized crystals accompanied by the decrease in the number of larger crystals after laser irradiance. Based on these observations, one expects that in samples with predominantly larger crystals a smaller portion of crystals are sufficiently heated for complete volatilization. Therefore, the MALDI-MS signal from larger crystals would depend on the number of guest molecules incorporated in the desorbed layer of the crystal. Selective volatilization of the smaller crystals can also explain that in many cases no visually observable damage to MALDI targets is observed after laser exposure.
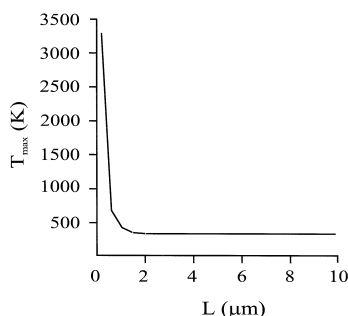
Fig. 6. Maximum calculated axial surface temperatures in a finite slab as a function of layer thickness for a Gaussian surface source.

accounts for related sample preparation effects in this method. Both the images and the presented calculation of surface temperature suggest that shifting the crystal size distribution below a critical size limit may result in more efficient volatilization. As a result, methods that tend to form smaller crystals may provide more reproducible spectra.

Acknowledgements

The results of our investigations can be correlated to a previously developed model [18]. Evaluating Eqs. (2) and (3) for $r = 0$, $z = 0$ and different L sample thicknesses indicate that under similar laser irradiation conditions, the maximum surface temperature of thin layers increases markedly compared to their thicker counterparts (Fig. 6). The high maximum temperatures for small thicknesses correspond to transient superheating of the solid. This effect is related to the obstruction of heat conduction when the thickness of the layer becomes comparable to the heat conduction length. Under these circumstances the energy deposited by the laser cannot be freely dissipated by heat conduction into the layer. Generalizing these results to three dimensions we can infer that the surface temperature of smaller crystals becomes greater than that of crystals with larger dimensions due to the hindrance of heat dissipation. The results of these calculations may explain the selective volatilization of smaller crystallites and the presence of two different morphological effects as a function of crystallite size. Our laser heating simulations suggest that crystals below a critical size will become completely volatilized. If the majority of the crystals in the size distribution are small enough to fall into this category, the possibility of observing reproducible MALDI signal is greater. Sample preparation methods that lead to the formation of samples with smaller crystals have been shown to produce better reproducibility [11], improved resolution, higher sensitivity [9], and adequate S/N in fewer laser shots [12].

The presented imaging studies point to the importance of crystal size distributions in MALDI-MS and

References

[1] R.C. Beavis, J.N. Bridson, J. Phys. D 26 (1993) 442.

[2] K. Schneider, B.T. Chait, Org. Mass Spectrom. 28 (1993) 1353.

[3] J.A. Carroll, R.C. Beavis, in: J.C. Miller, R.F. Haglund Jr. (Eds.), Laser Desorption and Ablation in the Series Experimental Methods in the Physical Sciences, Chap. 7, Web site: http://128.122.10.3/MALDI/ChemPhysMan.htm.

[4] A. Westman, PhD thesis, Chap. 7, University of Uppsala, Sweden, 1994.

[5] A. Westman, P. Demirev, T. Huth-Fehre, J. Bielawski, B.U.R. Sundqvist, Int. J. Mass Spectrom. Ion Processes 130 (1994) 107.

[6] M. Karas, F. Hillenkamp, Anal. Chem. 60 (1988) 2299.

[7] S.J. Doktycz, P.J. Savickas, D.A. Kruegger, Rapid Commun. Mass Spectrom. 5 (1991) 145.

[8] A.J. Nicola, A.I. Gusev, A. Proctor, E.K. Jackson, D.M. Hercules, Rapid Commun. Mass Spectrom. 9 (1995) 1164.

[9] O. Vorm, P. Roepstorff, M. Mann, Anal. Chem. 66 (1994) 3281.

[10] F. Xiang, R.C. Beavis, Rapid Commun. Mass Spectrom. 8 (1994) 199.

[11] D.A. Allwood, I.K. Perera, J. Perkins, P.E. Dyer, G.A. Oldershaw, Appl. Surf. Sci. 103 (1996) 231.

[12] S.R. Weinberger, K.O. Boernsen, J.W. Finch, V. Robertson, B.D. Musselman, in: Proceedings of the 41st ASMS Conference on Mass Spectrometry and Allied Topics, San Francisco, CA, 1993, p. 775.

[13] I.K. Perera, J. Perkins, S. Kantartzoglou, Rapid Commun. Mass Spectrom. 9 (1993) 180.

[14] I.K. Perera, S. Kantartzoglou, P.E. Dyer, Int. J. Mass Spectrom. Ion Processes 156 (1996) 151.

[15] S.L. Cohen, B.T. Chait, Anal. Chem. 68 (1996) 31.
[16] B. Lindner, Int. J. Mass Spectrom. Ion Processes 103 (1991) 203.
[17] J. Axelsson, A.M. Hoberg, C. Waterson, P. Myatt, G.L. Shield, J. Varney, D.M. Haddleton, P.J. Derrick, Rapid Commun. Mass Spectrom. 11 (1997) 209.
[18] A. Vertes, in: Proceedings of the 42nd ASMS Conference on Mass Spectrometry and Allied Topics, Chicago, IL, 1994, p. 2.
[19] W. Ens, Y. Mao, F. Mayer, K.G. Standing, Rapid Commun. Mass Spectrom. 5 (1991) 117.
[20] E.L. Crow, K. Shimizu (Eds.), Lognormal Distribution, Theory and Applications, Marcel Dekker, New York, 1988, pp. 1–22.
[21] M. von Allmen, Laser-Beam Interactions with Materials, Springer, Germany, 1987, pp. 53–58.
[22] A. Vertes, G. Irinyi, R. Gijbels, Anal. Chem. 65 (1993) 2389.